# Aharonov-Bohm ring with a side-coupled atomic cluster: Magnetotransport and the selective switching effect

Supriya Jana and Arunava Chakrabarti
*Department of Physics, University of Kalyani, Kalyani, West Bengal 741 235, India*
(Received 22 December 2007; published 9 April 2008)

We report the electronic transmission properties of a simple tight binding Aharonov-Bohm ring threaded by a magnetic flux to one arm of which a finite cluster of atoms has been attached from one side. We demonstrate that, by suitably choosing the number of scatterers in each arm of the quantum ring, the transmission across the ring can be completely blocked when the ring is decoupled from the atomic cluster and the flux threading the ring becomes equal to half the fundamental flux quantum. A transmission resonance then immediately occurs as the coupling between the ring and the impurity cluster is switched "on." It is shown that narrow transmission resonances precisely occur at the eigenvalues of the side-coupled chain of atoms. The "switching" effect can be observed either for all the eigenvalues of the isolated atomic cluster, or for a selected set of them, depending on the number of scatterers in the arms of the ring. The ring-dot coupling can be gradually increased to completely suppress the oscillations in the magnetotransmission. However, the suppression can lead either to a complete transparency or no transmission at all, occasionally accompanied by a reversal of phase at special values of the magnetic flux.

DOI: 10.1103/PhysRevB.77.155310 PACS number(s): 73.63.Kv, 73.21.La, 73.23.Ra, 73.63.Nm

## I. INTRODUCTION

Simple tight binding models of mesoscopic systems have been quite extensively studied in recent times[1–20] with a view to understand the basic features of electronic transport in quantum dots (QDs) or the magnetotransport in closed loop geometries such as an Aharonov-Bohm (AB) ring. One reason behind such model studies is definitely the simple geometry of the models, which enables one to derive exact results and to look into the possible causes of certain salient features observed in the transport properties of real life small scale semiconducting or metallic systems. The other reason can be attributed to the immense success of nanotechnology and the use of precision instruments such as a scanning tunneling microscope which can be used to build low dimensional nanostructures with tailor-made geometries. One such geometry, which will be our concern in this paper, is an AB ring threaded by a magnetic flux $\Phi$ and with a finite segment of $N$ atomic sites attached to one arm of the ring at an arbitrary point.

The central feature of electron transport across an AB ring is the periodic oscillation in the magnetoconductance whenever the phase coherence length exceeds the dimension of the sample.[21] Büttiker *et al.*[22] provided an early formulation of the problem. The transport in such a closed geometry was readdressed by Gefen *et al.*[23] who obtained an exact expression for the two-terminal conductance across the ring. By using a discrete tight binding formulation, the two-terminal conductance was also examined by D'Amato *et al.*[24] and, subsequently, by Aldea *et al.*[25] A nontrivial change in the transport of an AB ring is observed when the ring contains a QD either embedded in an arm or side coupled to it.[26–28] Motivated by the experiment of Yacoby *et al.*,[26] Yeyati and Büttiker[29] prescribed an exact formulation of the magnetoconductance of an AB ring with a QD embedded in its arm. A similar problem with a multiterminal geometry was later addressed by Kang.[30] The QD-AB ring hybrid system also received attention in relatively recent experiments by Meier *et al.*[31] and Kobayashi and co-workers,[32,33] with a focus on the study of single electron charging and suppression of AB oscillations[31] and the Fano resonance[34,35] in the magnetoconductance.

In a quantum dot, discrete energy levels arise as a consequence of confinement of electrons in all three directions. This has inspired a considerable number of theoretical works involving a discrete lattice of the so-called "single level" QDs,[1] mimicked by "atomic" sites arranged either in an open geometrical arrangement or in a closed AB ring within a tight binding formalism. For example, QDs, single or in an array, side coupled to an open chain have already received attention in the context of the Kondo effect,[3] one electron transport,[6,7,12] and the Dicke effect.[9] The prospect of engineering Fano resonances,[13–16] design of spin filters,[34] and the localization-delocalization problem[4] in a series of atomic clusters side coupled to an infinite lattice have also been discussed in detail.

Motivated by such simple models which, in spite of their simplicity, bring out the rich quantum coherence effects exhibited by a mesoscopic system, we revisit the problem of magnetotransport in an AB ring threaded by a magnetic flux, but now with a chain of $N$ atomic sites (an array of *single level QDs*) attached to one arm of the ring. In spite of the previous studies, we believe that the interplay of the closed loop geometry and the eigenvalue spectrum of the dangling QD array is little studied and is likely to provide features in the electronic transport, which might throw some light on the potential of such systems as quantum devices. This is our main objective.

We focus on the role of the ring-dot coupling, in particular, and come across several interesting results. For example, it is found that the ring-dot system displays a "switching" action for small values of the ring-dot coupling at selected energies of the electron when the flux penetrating the ring is $\Phi=\Phi_0/2$. The energy values (at which the switching takes

 

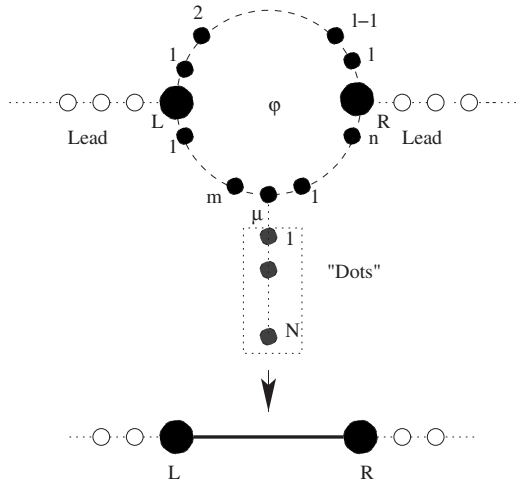


FIG. 1. The quantum ring and the side-coupled chain of quantum dots. The sites $L$ and $R$ (bigger solid circles) mark the left and the right junctions with the leads, and the site marked by $\mu$ is the "connecting" point of the side-coupled chain.

place), for a given size of the QD array coupled to the ring, belong to the set of eigenvalues of the isolated QD array and depend on the number of scatterers in the upper and the lower arms of the ring. A gradual increase in the ring-dot coupling suppresses the AB oscillations and is accompanied by occasional transmission phase reversals at specific values of the magnetic flux.

In what follows, we present the model and the method in Sec. II. Section III contains the results and the related discussion, and we draw conclusions in Sec. IV.

## II. MODEL AND METHOD

We begin by referring to Fig. 1. The ring contains $l$ atoms in the upper arm, excluding the sites marked by $L$ and $R$ where the leads join the ring. The site marked by $\mu$ in the lower arm is the point where the dangling QD chain is attached. There are $m$ sites to the left of $\mu$ and $n$ sites to its right. Changing $m$ and $n$ therefore shifts the location of the attachment of the "defect" chain. The Hamiltonian of the lead-ring-dot-lead system, in the standard tight binding form, is written as

$$H = H_{lead} + H_{ring} + H_{dot} + H_{ring\text{-}dot} + H_{ring\text{-}lead}, \tag{1}$$

where

$$H_{lead} = \epsilon_0 \sum_{i=-\infty}^{L-1} c_i^\dagger c_i + \epsilon_0 \sum_{i=R+1}^{\infty} c_i^\dagger c_i + t_0 \sum_{\langle ij \rangle} c_i^\dagger c_j,$$

$$H_{ring} = \epsilon_L r_L^\dagger r_L + \epsilon_R r_R^\dagger r_R + t_0 \exp(i\gamma) \sum_{\langle ij \rangle} r_i^\dagger r_j + \text{H.c.},$$

$$H_{dot} = \sum_{i=1}^{N} \epsilon_i d_i^\dagger d_i + t_0 \sum_{i=1}^{N-1} d_i^\dagger d_j + \text{H.c.},$$

$$H_{ring\text{-}dot} = \lambda (r_\mu^\dagger d_1 + \text{H.c.}),$$

$$H_{ring\text{-}lead} = t_0 (r_L^\dagger c_{L-1} + r_R^\dagger c_{R+1}). \tag{2}$$

In the above, $c^\dagger(c)$, $r^\dagger(r)$, and $d^\dagger(d)$ represent the creation (annihilation) operators for the leads, the ring, and the QD chain, respectively. $r_L(r_L^\dagger)$ and $r_R(r_R^\dagger)$ represent the same at the lead-ring connecting sites $L$ and $R$, respectively. The on-site potential at the leads, in the QD chain and in the bulk of the ring, is taken to be $\epsilon_0$ for every site including the site marked by $\mu$. The lead-ring connecting sites have been assigned the on-site potentials $\epsilon_L$ and $\epsilon_R$, respectively. The amplitude of the hopping integral is taken to be $t_0$ throughout except the hopping from the site $\mu$ in the ring to the first site of the QD chain, which has been symbolized as $\lambda$ and represents the "strength" of coupling between the ring and the QD array. $\gamma$ is given by $\gamma = 2\pi\Phi/(l+m+n+1)\Phi_0$, where $\Phi$ is the flux threading the ring, and $\Phi_0 = hc/e$ is the fundamental flux quantum. The task of solving the Schrödinger equation to obtain the stationary states of the system can be reduced to an equivalent problem of solving a set of the following difference equations.

For the sites $L$ and $R$ at the ring-lead junctions,

$$(E - \epsilon_L)\psi_L = t_0 e^{i\gamma}\psi_{1,\mathcal{U}} + t_0 e^{-i\gamma}\psi_{1,\mathcal{L}} + t_0\psi_{L-1},$$

$$(E - \epsilon_R)\psi_R = t_0 e^{-i\gamma}\psi_{l,\mathcal{U}} + t_0 e^{i\gamma}\psi_{m+n+1,\mathcal{L}} + t_0\psi_{R+1}. \tag{3}$$

In the above, $\psi_{L-1}$ and $\psi_{R+1}$ represent the amplitudes of the wave function at the sites on the lead, which are closest to the points $L$ and $R$, and $\mathcal{U}$ and $\mathcal{L}$ in the subscripts refer to the "upper" and the "lower" arms, respectively.

For the sites in the bulk of the ring, the equations are

$$(E - \epsilon_0)\psi_{j,\mathcal{U}} = t_0 e^{-i\gamma}\psi_{j-1,\mathcal{U}} + t_0 e^{i\gamma}\psi_{j+1,\mathcal{U}},$$

$$(E - \epsilon_0)\psi_{j,\mathcal{L}} = t_0 e^{i\gamma}\psi_{j-1,\mathcal{L}} + t_0 e^{-i\gamma}\psi_{j+1,\mathcal{L}}, \tag{4}$$

where, by $j+1$ and $j-1$, we symbolize the sites to the right and to the left of the $j$th site in any arm of the ring.

For the site marked by $\mu$ in the lower arm of the ring, the equation is

$$(E - \epsilon_0)\psi_{\mu,\mathcal{L}} = t_0 e^{i\gamma}\psi_{\mu-1,\mathcal{L}} + t_0 e^{-i\gamma}\psi_{\mu+1,\mathcal{L}}, \tag{5}$$

where $\mu \pm 1$ imply the sites to the right and to the left of the site marked by $\mu$, respectively. Finally, for the QD array, we have the following set of difference equations:

$$(E - \epsilon_1)\psi_1 = \lambda\psi_\mu + t_0\psi_2,$$

$$(E - \epsilon_j)\psi_j = t_0\psi_{j-1} + t_0\psi_{j+1},$$

$$(E - \epsilon_N)\psi_N = t_0\psi_{N-1}, \tag{6}$$

where the central set of equations above refer to the bulk sites, viz., $j = 2, \ldots, N-1$ in the QD array.

The process of calculating the transmission coefficient across such a ring-dot system consists of the following steps. First, the dangling QD chain is "wrapped" into an effective site by decimating the amplitudes $\psi_2$ to $\psi_N$ from Eq. (6). The renormalized on-site potential of the first site of the QD array is given by[15]

$$\tilde{\epsilon} = \epsilon_0 + \frac{t_0 U_{N-3}(x)}{U_{N-2}(x)} + \frac{t_0^2}{U_{N-2}^2(x)} \frac{1}{E - \epsilon_0 - \frac{t_0 U_{N-3}(x)}{U_{N-2}(x)}} \tag{7}$$

for $N \geqslant 2$. For $N=1$, we simply have $\tilde{\epsilon} = \epsilon_0 + \lambda^2/(E-\epsilon_0)$. Here, $x=(E-\epsilon_0)/2t_0$ and $U_N(x)$ is the $N$th order Chebyshev polynomial of the second kind, with $U_0=1$ and $U_{-1}=0$.[36] This "effective" site is coupled to the site marked by $\mu$ in the lower arm of the ring via a hopping integral $\lambda$. In the second step, the effective site with on-site potential is further "folded" back into the site $\mu$, whose renormalized on-site potential now reads[15]

$$\epsilon^* = \epsilon_0 + \frac{\lambda^2}{E - \tilde{\epsilon}}. \tag{8}$$

We now have a ring with $l$ atoms in the upper arm and an effective site at position $\mu$ in the lower arm, flanked by $m$ atoms on its left and $n$ atoms on the right, so that there is a total of $m+n+1$ atoms in the lower arm. This is just the case of a QD with an energy dependent on-site potential embedded in an arm of an AB ring. In the final step, all the $l+m+n+1$ atoms are decimated by using the set of appropriate difference equations [Eqs. (3) and (4)] to reduce the ring into an effective *diatomic molecule* (Fig. 1). The renormalized values of the on-site potential at the two extremeties of the molecule are given by

$$\tilde{\epsilon}_L = \epsilon_0 + t_0\left(\frac{U_{l-1}}{U_l} + \frac{U_{m-1}}{U_m}\right) + \frac{t_0^2}{U_m^2} F(E,\lambda,m,n),$$

$$\tilde{\epsilon}_R = \epsilon_0 + t_0\left(\frac{U_{l-1}}{U_l} + \frac{U_{n-1}}{U_n}\right) + \frac{t_0^2}{U_n^2} F(E,\lambda,m,n), \tag{9}$$

where for a fixed set of $\epsilon_0$ and $t_0$,

$$F(E,\lambda,m,n) = \left[E - \epsilon^* - t_0\left(\frac{U_{m-1}}{U_m} + \frac{U_{n-1}}{U_n}\right)\right]^{-1}. \tag{10}$$

The time reversal symmetry of the hopping integral between the atoms at $L$ and $R$ of the diatomic molecule is broken due to the flux threading the ring and is given by

$$t_F = \frac{t_0}{U_l} e^{i(l+1)\gamma} + \frac{t_0^2}{U_m U_n} F(E,\lambda,m,n) e^{-i(m+n+2)\gamma} \tag{11}$$

for the *forward* hopping from $L$ to $R$ and by $t_B = t_F^*$ for the *backward* hopping from $R$ to $L$. The transmission coefficient across the effective diatomic molecule is given by[37]

$$T = \frac{4 \sin^2 qa}{|M_{12} - M_{21} + (M_{11} - M_{22})\cos qa|^2 + |M_{11} + M_{22}|^2 \sin^2 qa}, \tag{12}$$

where $a$ is the lattice constant in the leads, taken to be equal to 1 throughout the calculation. In what follws, we discuss various aspects of the electronic transmission across the ring-QD array system. We fix the on-site potential at all sites, including the QD chain, as $\epsilon_0$ and the hopping integrals have been kept equal to $t_0$ throughout, except the ring-QD array coupling $\lambda$. The defect that we hang from an otherwise perfect ring is thus only of a topological nature.

## III. RESULTS AND DISCUSSIONS

### A. Suppression of Aharonov-Bohm oscillations

In all transmission profiles, the ring-dot coupling $\lambda$ plays a crucial role. The first effect that we present is a suppression of the AB oscillations as a function of $\lambda$. We choose the energy $E$ from a specially selected set obtained by solving the equation $E-\tilde{\epsilon}=0$. For these $E$ values, the suppression of the AB oscillations can be directly worked out from our formulation. It is to be appreciated that the eigenvalues of the isolated quantum dot array are obtained by solving the polynomial equation $E-\tilde{\epsilon}=0$.[13–15] We select any one of the roots, name it $\tilde{\epsilon}_0$, and fix $\lambda \neq 0$. This last condition is important.

A close look at the expression of $\epsilon^*$ reveals that for $E=\tilde{\epsilon}_0$ (in fact, for any real root of the equation $E-\tilde{\epsilon}=0$), we get $\epsilon^*=\infty$. This leads to the following reduced forms of $\epsilon_L$, $\epsilon_R$, and $t_F$ $(=t_B^*)$:

$$\tilde{\epsilon}_L = \epsilon_0 + t_0\left(\frac{U_{l-1}}{U_l} + \frac{U_{m-1}}{U_m}\right),$$

$$\tilde{\epsilon}_R = \epsilon_0 + t_0\left(\frac{U_{l-1}}{U_l} + \frac{U_{n-1}}{U_n}\right),$$

$$t_F = \frac{t_0}{U_l} e^{i(l+1)\gamma}. \tag{13}$$

We observe that the ring-dot coupling $\lambda$ does not appear in any of these expressions. This is because of the selection $E=\tilde{\epsilon}_0$ and a nonzero $\lambda$, however, is small. Let us now define $\cos(qa) = (E-\epsilon_0)/2t_0 = (\tilde{\epsilon}_0 - \epsilon_0)/2t_0 = \delta/2t_0$, $\tilde{\epsilon}_0 - \tilde{\epsilon}_L = \xi_1$, and $\tilde{\epsilon}_0 - \tilde{\epsilon}_R = \xi_2$. With these, the transfer matrix elements for the diatomic molecule read

$$M_{11} = \left[\frac{\xi_1 \xi_2 U_l}{t_0^2} - \frac{1}{U_l}\right] e^{-i(l+1)\gamma},$$

$$M_{12} = -\frac{\xi_2 U_l}{t_0} e^{-i(l+1)\gamma},$$

$$M_{21} = \frac{\xi_1 U_l}{t_0} e^{-i(l+1)\gamma},$$

$$M_{22} = -U_l e^{-i(l+1)\gamma}. \tag{14}$$

Finally, the transmission coefficient is given by

$$T = \frac{4\left[1 - \frac{\delta^2}{4t_0^2}\right]}{|d_1|^2 + |d_2|^2}, \tag{15}$$

where

$$d_1 = \frac{e^{-i(l+1)\gamma}}{t_0}\left[\left(\frac{\xi_1\xi_2 U_l}{t_0^2} + \frac{U_l^2 - 1}{U_l}\right)\frac{\delta}{2} - (\xi_1 + \xi_2)U_l\right],$$

$$d_2 = e^{-i(l+1)\gamma}\left(\frac{\xi_1\xi_2 U_l}{t_0^2} - \frac{U_l^2 + 1}{U_l}\right)\sqrt{1 - \frac{\delta^2}{4t_0^2}}. \quad (16)$$

As we observe, $|d_1|^2$ and $|d_2|^2$ and hence $T$ are independent of the flux. That is, the AB oscillations are suppressed whenever the Fermi energy coincides with any of the discrete eigenvalues of the isolated QD array.

In view of the above calculation, a few pertinent observations should be given importance. Let us slightly detune $E$ from an eigenvalue of the QD array. That is, let us set $E - \tilde{\epsilon}_0 = \Delta$, $\Delta$ being very small. How does the shape of the AB oscillation get altered in the neighborhood of $E = \tilde{\epsilon}_0$? In this case, we have

$$\epsilon^* = \epsilon_0 + \frac{\lambda^2}{\Delta}. \quad (17)$$

Clearly, if $\lambda \neq 0$, but very very small so that $\lambda^2 \sim \mathcal{O}(\Delta)$, then the analysis as given above is not valid, as $\epsilon^*$ is not *infinity* anymore. As a result, we shall observe AB oscillations in the transmission spectrum in general. If we gradually increase the value of $\lambda$ so that $\Delta \ll \lambda$, or even smaller, then we essentially keep on making $\lambda^2/\Delta$ and hence $\epsilon^*$ larger and larger. This results in the gradual suppression of the amplitude of the AB oscillations, and finally, when $\lambda^2/\Delta$ becomes a very large number (dictated by the machine precision), the transmission coefficient ($T$) becomes independent of the flux threading the ring. AB oscillations completely disappear.

An interesting feature of the AB oscillations in such cases is that a gradual increase in the value of $\lambda$ can lead either to $T=1$ [Fig. 2(a)] or to $T=0$ [Figs. 2(b) and 2(c)]. This depends on the combination of the size of the ring (i.e., on $l$, $m$, and $n$) and the length of the QD array ($N$). In every case, however, the progress toward $T=1$ or $T=0$ is accompanied by a gradual suppression of the AB oscillations. Most interestingly, for a set of values of $l$, $m$, $n$, and $N$, the phase of the AB oscillations is reversed at specific values of the magnetic flux as soon as $\lambda$ exceeds some "critical" value. Incidentally, a similar observation in a simpler geometry was reported by Kubala and König as well.[1] The present cases are depicted in Figs. 2(b) and 2(c), where the reversal is observed at $\Phi = \Phi_0/2$ and $3\Phi_0/2$ (odd multiple of $\Phi_0/2$ in general). However, with different combinations of $l$, $m$, $n$, and $N$, the reversal can take place at other flux values as well, for example, at $\Phi=0$ and $\Phi=\Phi_0$. We have not been able to obtain an exact criterion for the phase reversal. However, an extensive numerical search has revealed that this is true for various combinations of the size of the ring and the length of the QD array.

Before ending, it should be mentioned that the flux independence that we have discussed above is basically caused by the divergence of $\epsilon^*$ at special energies. This divergence can also be achieved for any arbitrary energy other than the eigenvalues of the isolated QD array by letting $\lambda \to \infty$. Such a situation, as we have carefully observed, but do not report here to save space, leads to a flux independent $T$-$E$ spectrum.

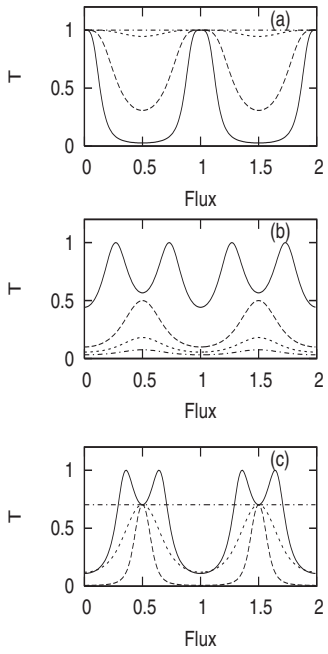


FIG. 2. The gradual suppression of AB oscillations in the transmission spectrum as the ring-dot coupling increases. (a) $E=10^{-6}$, $l=13$, $m=n=6$, and $N=5$. Here, $\lambda=0.001$ (solid), 0.002 (dashed), 0.005 (dotted), and 0.1 (dot-dash). (b) $E=10^{-6}$, $L=7$, $m=3$, $n=8$, and $N=7$. $\lambda=0.001$ (solid), 0.004 (dashed), 0.005 (dotted), and 0.006 (dot-dash). (c) $E=0.618\,011\,988$, $l=9$, $m=3$, $n=8$, and $N=4$. The values of $\lambda$ are 0.001 (solid), 0.007 (dashed), 0.01 (dotted), and 0.5 (dot-dash), respectively. Other parameters are $\epsilon_0=0$ and $t_0=1$, and the energy and $\lambda$ are measured in units of $t_0$, and the flux is measured in units of $\Phi_0$.

### B. Selective switching

At first, we note that, for $l=m+n+1$, i.e., for an equal number ($l$) atoms in the two arms, and with $\lambda=0$, the $L$-$R$ hopping integral in the effective diatomic molecule is real and reads

$$t_F = \frac{2t_0}{U_l}\cos\left(\frac{\pi\Phi}{\Phi_0}\right), \quad (18)$$

where $t_B$ is, of course, equal to $t_F$. It is now clear that for $\Phi=\Phi_0/2$, the effective hopping integral becomes zero, resulting in $T=0$ (an antiresonance), independent of the energy of the electron. As soon as the ring-dot coupling $\lambda$ assumes a nonzero value, interesting transmission behavior is observed. To get a clearer understanding, we refer to Fig. 3, which is a

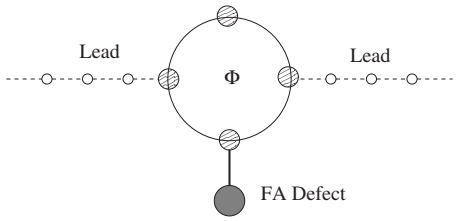


FIG. 3. A simple four-site ring with a single Fano-Anderson (FA) defect attached to it.

ring with just one atom in both the lower and the upper arms with a single QD with an on-site potential $\epsilon_D$ coupled to the atom in the lower arm. This is a simple modification of the model used by Kubala and König.[1] For this simple geometry, with $\lambda \neq 0$, we get

$$\tilde{\epsilon}_L = \epsilon_0 + \frac{t_0^2}{E-\epsilon_0} + \frac{t_0^2(E-\epsilon_D)}{(E-\epsilon_0)(E-\epsilon_D)-\lambda^2},$$

$$t_F = (-i)t_0^2 \frac{\lambda^2}{(E-\epsilon_0)[(E-\epsilon_0)(E-\epsilon_D)-\lambda^2]}, \tag{19}$$

with $\tilde{\epsilon}_R = \tilde{\epsilon}_L$ and $t_B = t_F^*$. By using these, one can work out the transfer matrix elements for the diatomic molecule, in the limit $E \to \epsilon_D$, to be equal to

$$\lim_{E\to\epsilon_D} M_{11} = \frac{-i\delta(2t_0^2-\delta^2)}{t_0^3},$$

$$\lim_{E\to\epsilon_D} M_{12} = \frac{-i(t_0^2-\delta^2)}{t_0^2},$$

$$\lim_{E\to\epsilon_D} M_{21} = \frac{i\delta(2t_0^2-\delta^2)}{t_0^3},$$

$$\lim_{E\to\epsilon_D} M_{22} = \frac{-i\delta}{t_0}, \tag{20}$$

where $\delta = \epsilon_0 - \epsilon_D$. Inserting these values in the formula for the transmission coefficient, it is observed that $T=1$ for $E=\epsilon_D$ with any $\lambda \neq 0$. That is, the presence of a finite ring-dot coupling, however small, triggers ballistic transmission across the ring.

With an arbitrary number of scatterers in either arm of the ring, and the QD array extending beyond one atom, the situation is nontrivial and closed form expressions look extremely cumbersome to deal with. We have conducted an extensive and careful numerical investigation to examine several cases. Here, details of a specific case are given which reflect the generic features of the *selective switching* effect that we wish to highlight.

We choose a situation where the QD array contains, for example, five atoms ($N=5$). The on-site potential $\epsilon_0$ and the hopping integral $t_0$ are set equal to zero and unity everywhere, including the QD array. We set the magnetic flux $\Phi = \Phi_0/2$ and select $l=2m+1$ and $m=n$. The five-site QD chain is now diagonalized to get the eigenvalues 0, $\pm 1$, and $\pm\sqrt{3}$. With $\lambda$ set equal to zero, as discussed before, we get $T=0$ irrespective of energy $E$. Interestingly, it is found that, by choosing a small nonzero value of $\lambda$ and an appropriate set of values for $l$, $m$, and $n$, but always satisfying the requirement $l=2m+1$ and $m=n$, it is possible to make the ring-dot system *completely transparent* to an incoming electron when its energy becomes equal to some or all of the eigenvalues of the five-site QD array. The transmission at any energy outside the set of five eigenvalues mentioned above can be completely suppressed if $\lambda$ is kept small enough. However, a gradual increase in the value of $\lambda$ gives rise to secondary transmission peaks as the ring more strongly "interacts" with the QD. These secondary peaks finally settle into bands of transmission separated by transmission dips, as a result of quantum interference. The important thing to appreciate is that whether we observe complete transparency at a subset of the eigenvalues or for all of them depends strongly on the mutual tuning of the values of the ring-dot coupling $\lambda$ and $l$, $m$, and $n$. Figure 4 displays the selective switching action when the QD array contains three and five sites, respectively [Figs. 4(a) and 4(b)]. In Fig. 4(a), setting $\lambda=0.08$ and attaching the array to an $(l,m,n)=(1,0,0)$ ring (like the one shown in Fig. 2), we see that the transmission coefficient is unity (or very close to it) only when energy $E$ is equal to the three eigenvalues of the isolated three-dot array, viz., at $E=0$ and $\pm\sqrt{2}$. On the other hand, with $N=5$ [Fig. 4(b)], with $l=17$, $m=n=8$, and $\lambda=0.04$, transmission is triggered only at three of the five eigenvalues. The scenario of course changes as the parameters are varied, keeping $\lambda$ small. However, the "smallness" of $\lambda$ is to be selected by a trial method, at least so far as we have checked. In Table I, we provide a list of such selective values for which $T=1$ (or very close to it) at $\Phi=\Phi_0/2$.

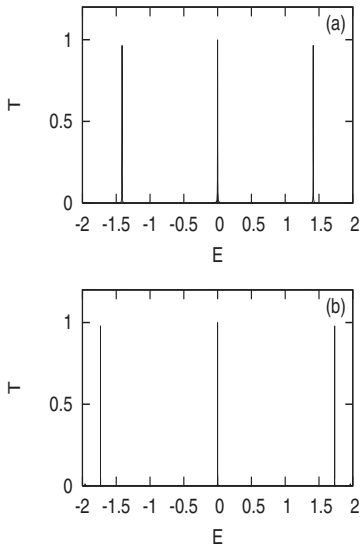


FIG. 4. Selective switching effect at $\Phi=\Phi_0/2$ for a QD array of (a) three sites and (b) five sites. In (a), we have taken $l=1$, $m=n=0$, and $\lambda=0.08$. Three transmission peaks at three distinct eigenvalues $E=0$ and $\pm\sqrt{2}$ of the isolated three-site QD chain are visible. In (b), $l=17$, $m=n=8$, $N=5$, and $\lambda=0.04$. Peaks appear at $E=0, \pm\sqrt{3}$ and transmission at two other eigenvalues of the isolated QD chain, viz., at $E=\pm 1$ are blocked.

Before we end, it should be noted that the geometry dealt with in the present communication can equivalently be thought of as a discrete part (the lower arm plus the QD array) to an infinite linear chain (the left lead plus the upper arm plus the right lead). Considering no magnetic field, we expect Fano line shapes in the transmission spectrum as a result of an "interaction" of the discrete spectrum of the lower parts with the continuous spectrum offered by the upper section.[13,16] Indeed, there are such line shapes in the transmission resonances, which, however, get masked due to quantum interference as we take larger and larger sizes of the ring as well as the QD array.

TABLE I. Some typical combinations of $l$, $m$, and $n$ and the ring-dot coupling $\lambda$ that give rise to selective switching at $\Phi=\Phi_0/2$. $k$ is a positive integer.

| $(l,m,n)$ | Typical value of $\lambda$ | $T\sim 1$ at $E=$ |
|---|---|---|
| $(12k-1,6k-1,6k-1)$ | Arbitrary | No peak at all |
| $(12k-7,6k-4,6k-4)$ | 0.04 | $0, \pm\sqrt{3}$ |
| $(12k-5,6k-3,6k-3)$ | 0.04–0.045 | $\pm 1, \pm\sqrt{3}$ |
| $(12k+3,6k+1,6k+1)$ | 0.04–0.045 | $\pm 1, \pm\sqrt{3}$ |
| $(12k-11,6k-6,6k-6)$ | 0.05–0.10 | $0, \pm 1, \pm\sqrt{3}$ |
| $(12k-3,6k-2,6k-2)$ | 0.05–0.10 | $0, \pm 1, \pm\sqrt{3}$ |

## IV. CONCLUSION

We have addressed the issue of transmission across an Aharonov-Bohm ring with a dangling chain of single level quantum dots within a tight binding formalism. In the presence of a magnetic flux threading the ring, we discuss the role of the ring-dot coupling in controlling the profile of transmission oscillations. The central feature is a suppression of the AB oscillations with occasional reversal of phase at specific values of the flux. Most interestingly, it is found that a simultaneous adjustment of the number of scatterers in the arms of the ring and the ring-dot coupling can lead to a complete transparency of the system at some or all of the eigenvalues of the QD array. It is important to note that a bigger ring with large values of $l$, $m$, and $n$ (always satisfying the condition $m=n$, $l=2m+1$, and $\Phi=\Phi_0/2$) exhibits ballistic transmission $T=1$ for rather low values of the ring-dot coupling $\lambda$. This is because with a bigger ring, the coupled QD array stays far away from the junctions $L$ and $R$. The "end effects" are thus minimized. We have also tested these features with a QD array formed according to the quasiperiodic Fibonacci growth rule.[14] The essential features, such as the self-similarity in the electronic transmission, are also observed in the selective switching case. Such aspects will be discussed elsewhere.


[1] B. Kubala and J. König, Phys. Rev. B **65**, 245301 (2002).
[2] Z. Y. Zeng, F. Claro, and A. Pérez, Phys. Rev. B **65**, 085308 (2002).
[3] M. E. Torio, K. Hallberg, A. H. Ceccatto, and C. R. Proetto, Phys. Rev. B **65**, 085302 (2002).
[4] V. Pouthier and C. Girardet, Phys. Rev. B **66**, 115322 (2002).
[5] M. L. Ladrón de Guevara, F. Claro, and P. A. Orellana, Phys. Rev. B **67**, 195335 (2003).
[6] P. A. Orellana, F. Domínguez-Adame, I. Gómez, and M. L. Ladrón de Guevara, Phys. Rev. B **67**, 085321 (2003).
[7] A. Rodríguez, F. Domínguez-Adame, I. Gómez, and P. A. Orellana, Phys. Lett. A **320**, 242 (2003).
[8] Y.-J. Xiong and X.-T. Liang, Phys. Lett. A **330**, 307 (2004).
[9] P. A. Orellana, M. L. Ladrón de Guevara, and F. Claro, Phys. Rev. B **70**, 233315 (2004).
[10] I. Gómez, F. Domínguez-Adame, and P. Orellana, J. Phys.: Condens. Matter **16**, 1613 (2004).
[11] M. E. Torio, K. Hallberg, A. E. Miroshnichenko, and M. Titov, Eur. Phys. J. B **37**, 399 (2004).
[12] F. Domínguez-Adame, I. Gómez, P. A. Orellana, and M. L. Ladrón de Guevara, Microelectron. J. **35**, 87 (2004).
[13] A. E. Miroshnichenko and Y. S. Kivshar, Phys. Rev. E **72**, 056611 (2005).
[14] A. Chakrabarti, Phys. Rev. B **74**, 205315 (2006).
[15] A. Chakrabarti, Phys. Lett. A **366**, 507 (2007).
[16] A. E. Miroshnichenko, S. F. Mingaleev, S. Flach, and Y. S. Kivshar, Phys. Rev. E **71**, 036626 (2005).
[17] K. Bao and Y. Zheng, Phys. Rev. B **73**, 045306 (2006).
[18] H. Li, T. Lü, and P. Sun, Phys. Lett. A **343**, 403 (2005).
[19] M. Mardaani and K. Esfarjani, Physica E (Amsterdam) **27**, 227 (2005).
[20] Z.-B. He and Y.-J. Xiong, Phys. Lett. A **349**, 276 (2006).
[21] Y. Aharonov and D. Bohm, Phys. Rev. **115**, 485 (1959).
[22] M. Büttiker, Y. Imry, and R. Landauer, Phys. Lett. **96A**, 365 (1983).
[23] Y. Gefen, Y. Imry, and M. Ya. Azbel, Phys. Rev. Lett. **52**, 129 (1984).
[24] J. L. D'Amato, H. M. Pastawski, and J. F. Weisz, Phys. Rev. B **39**, 3554 (1989).
[25] A. Aldea, P. Gartner, and I. Corcotoi, Phys. Rev. B **45**, 14122 (1992).
[26] A. Yacoby, M. Heiblum, D. Mahalu, and H. Shtrikman, Phys. Rev. Lett. **74**, 4047 (1995).
[27] R. Schuster, E. Buks, M. Heiblum, D. Mahalu, V. Umansky, and H. Shtrikman, Nature (London) **385**, 417 (1997).
[28] A. W. Holleitner, C. R. Decker, H. Qin, K. Eberl, and R. H. Blick, Phys. Rev. Lett. **87**, 256802 (2001).
[29] A. L. Yeyati and M. Büttiker, Phys. Rev. B **52**, R14360 (1995).
[30] K. Kang, Phys. Rev. B **59**, 4608 (1999).
[31] L. Meier, A. Fuhrer, T. Ihn, K. Ensslin, W. Wegscheider, and M. Bichler, Phys. Rev. B **69**, 241302(R) (2004).
[32] K. Kobayashi, H. Aikawa, S. Katsumoto, and Y. Iye, Phys. Rev. Lett. **88**, 256806 (2002).
[33] K. Kobayashi, H. Aikawa, A. Sano, S. Katsumoto, and Y. Iye, Phys. Rev. B **70**, 035319 (2004).
[34] M. Lee and C. Bruder, Phys. Rev. B **73**, 085315 (2006); R. Wang and J.-Q. Liang, *ibid.* **74**, 144302 (2006).
[35] U. Fano, Phys. Rev. **124**, 1866 (1961).
[36] X. Wang, U. Grimm, and M. Schreiber, Phys. Rev. B **62**, 14020 (2000); J. Q. You and Q. B. Yang, J. Phys.: Condens. Matter **2**, 2093 (1990).
[37] A. D. Stone, J. D. Joannopoulos, and D. J. Chadi, Phys. Rev. B **24**, 5583 (1981).